

Transport of Freshwater into the Deep Ocean by the Conveyor

Scott J. Lehman, Daniel G. Wright[†] and Thomas F. Stocker^{††}

Woods Hole Oceanographic Inst., Woods Hole, MA

[†]Bedford Inst. of Oceanography, Dartmouth, NS, Canada

^{††}Lamont-Doherty Earth Observatory, Palisades, NY

Introduction:

The upper limb of the ocean's conveyor-belt circulation transports about one petawatt of heat across the equator in the Atlantic, of which approximately two-thirds is released to the atmosphere in the northern part of the basin as a result of deepwater formation. If all of this heat were taken up in melting ice, it would yield approximately 60,000 km³ of meltwater per year. Thus it is conceivable that peak deglacial melting rates of 5,000 -15,000 km³/yr (Fairbanks 1989) were achieved in response to sudden start-up or strengthening of the conveyor at the end of the last glaciation. Of course, a portion of the heat borne and released by the conveyor radiates to space, and much of the glacial ice at high elevation and high latitude must have been warmed prior to melting, consuming additional energy. But the point here is that even without sunlight at high latitudes, the transient heat gain associated with strengthening of the conveyor may have been sufficient or near-sufficient to account for the melting of the former ice sheets of the Northern Hemisphere. The potential role of the conveyor in melting the ice sheets is further underscored by Figure 1 showing that melting rates during the last deglaciation varied in accordance with the relative strength of the conveyor's upper limb (Lehman and Keigwin 1992). However, in most numerical ocean models the convection which drives the conveyor circulation is extremely sensitive to small changes in the freshwater balance at the surface (Maier-Reimer and Mikolajewicz 1989; Stocker et al. 1992). If such model sensitivities are close to being correct, it is difficult to understand how the conveyor remained "on" long enough to promote the large pulses of ice sheet melting seen in Figure 1.

A second observation of relevance to this problem is that high-resolution oxygen isotopic records in benthic foraminifera often show a two-step depletion in ¹⁸O during the deglaciation (cf. Duplessy et al 1981). A few records with exceptional resolution show that, at some locations, these steps correspond to two depletion "spikes" separated by an enrichment at approximately the time of the Younger Dryas (Figure 2). The low- $\delta^{18}\text{O}$ spikes may be explained in several ways: 1) by transient freshening of the deep ocean before and after the YD, 2) by transient warming of the deep ocean before and after the YD, or 3) by a change in the relationship between $\delta^{18}\text{O}$ and salinity in deepwater source areas before and after the YD, due either to a change in the amount and/or isotopic composition of glacial meltwater or in the extent

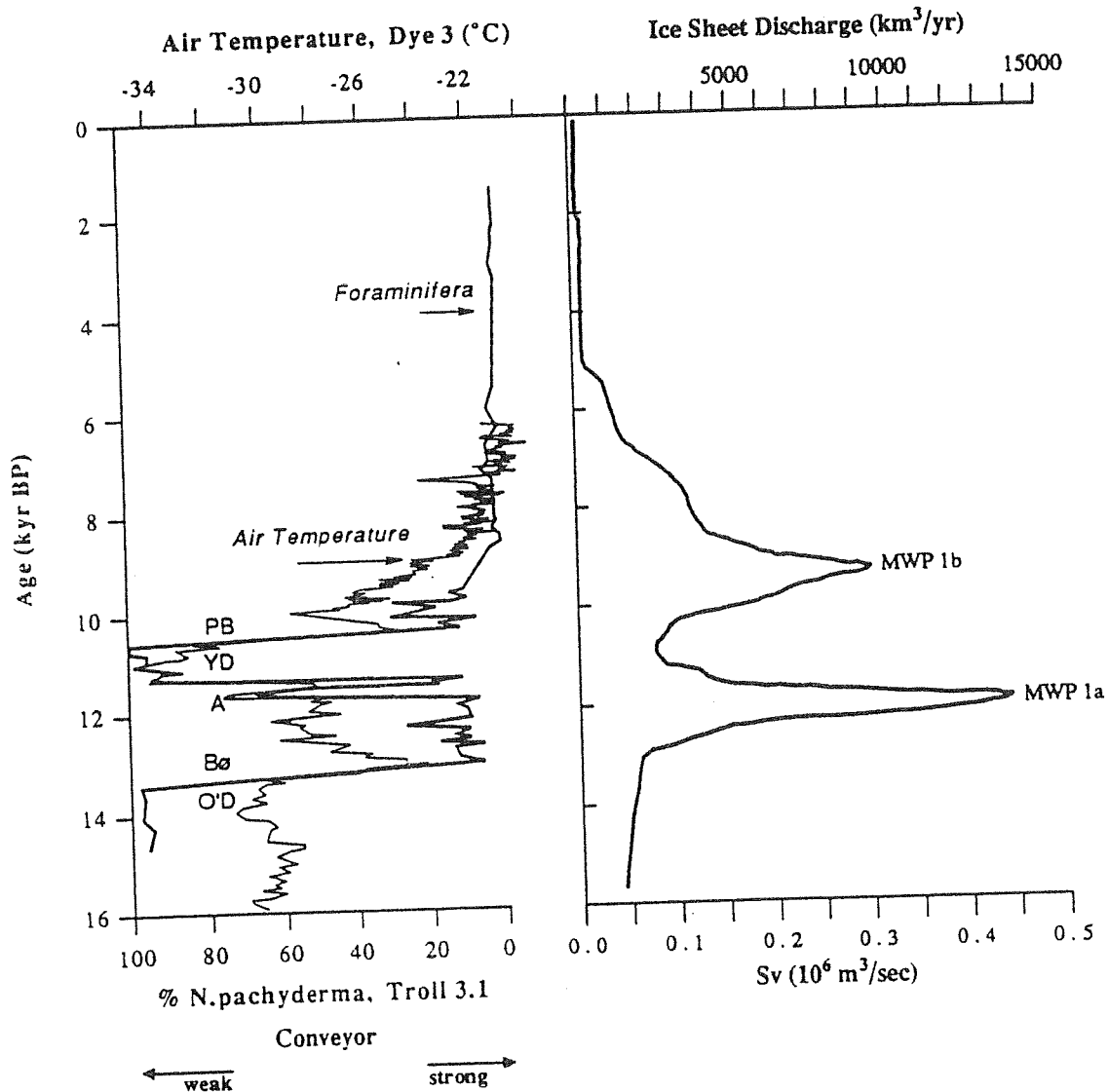


Figure 1: a) Percentage of the polar planktonic foraminifera in core Troll 3.1, from the southeastern Norwegian Sea, plotted to reservoir-corrected radiocarbon age and correlated to air temperature over Greenland as deduced from oxygen isotope variations in the Dye 3 ice core (ice core data are from Dansgaard et al 1982, correlations are explained in Lehman and Keigwin 1992). At times when percentages of the polar foraminifera were low, water temperatures and poleward flow of warm surface waters of the upper limb of the conveyor were greater. The close correspondence between changes in sea and air temperature suggests that variations in heat release by the conveyor controlled atmospheric temperatures, at least around the North Atlantic. Viewing the temperature records and the rate of ocean volume increase during the last deglaciation (from Fairbanks 1989) on a common timescale suggests that the conveyor also influenced ice sheet melting rates. The major trough in each record corresponds to the cold Younger Dryas (YD) period. The Oldest Dryas (O'D) - Bølling (Bø) transition marks the close of the full glacial. The conveyor was, in general, strong during the Bølling and Allerød (A), when ice sheet melting rates were rising. The Allerød is interrupted by a brief climatic reversal (previously referred to as the Intra-Allerød Cold Period by Lehman and Keigwin 1992) which we regard as marking the beginning of weakened conveyor circulation, atmospheric cooling, and the turnaround in icesheet melting rates. For the purposes of the present discussion, we equate these changes with the beginning of the YD event as seen in the model.

of brine-rejection by sea ice. As the timing of maximum ice sheet melting and benthic ^{18}O -depletion are similar, the simplest explanation is that $\delta^{18}\text{O}$ dropped temporarily when and where the rate of addition of ^{18}O -depleted meltwater exceeded the mixing capacity of the deep ocean. If the conveyor remained "on" during much or all of the periods of greatest melting, discrete pulses of meltwater may then have been advected into the deep ocean and recorded in the oxygen isotopic composition of benthic foraminifera. But, once again, if deepwater formation and conveyor-belt circulation in the real ocean had a sensitivity to freshening close to that of most models, how could such discrete pulses of freshwater have been advected to depth?

Wright and Stocker (this volume, hereafter WS-93) have recently made progress in addressing the sensitivity problem by investigating the dependence of the transient behavior of the thermohaline circulation on the strength of the hydrological cycle. Using a two-dimensional, coupled ocean - sea ice - atmosphere model forced by realistic deglacial meltwater fluxes, they identified a circulation response similar to the one inferred from Figure 1; thermohaline overturning collapsed following the first meltwater pulse, recovered spontaneously after about a millennium, and survived the second meltwater pulse. As this simulation produces a credible *history* of circulation change during the deglaciation, we use the same model in this study to explore the mechanisms by which ^{18}O -depleted freshwater is incorporated into the deep ocean. We find that some of the most significant changes in $\delta^{18}\text{O}$ of deepwater (and in carbonates precipitated in equilibrium with seawater) occur immediately upon re-establishment of the overturning circulation at the end of the YD. This occurs because, in these simulations, ^{18}O -depleted freshwater is sequestered at the ocean surface while the circulation is in the collapsed state. The accumulated freshwater is then advected rapidly through the deep Atlantic as the circulation abruptly recovers. Because the model has been spun-up under initial conditions approximating those of the present-day (or Allerød), this occurs only once in the simulations. In the real ocean the same phenomena may have occurred twice, first when the conveyor circulation increased following the last glaciation (at the transition from the Oldest Dryas to the Bølling), and then again at the termination of the YD. Thus, the "store and advect" mechanism may be useful in explaining the isotopic record in sediments, which commonly display two negative excursions, one before and the other after the YD.

The WS-93 Model and Younger Dryas Simulations:

WS-93 use a 2-D ocean model coupled to an Energy Balance Model of the atmosphere. The ocean model is based on the zonally-averaged balance-equations of mass, momentum, heat and salt developed in Wright and Stocker (1991) with extensions and simplifications presented in Wright and Stocker (1992). The model also includes a thermodynamic sea ice formulation based on that of Semtner (1976). All of the major ocean basins are resolved with a geometry as

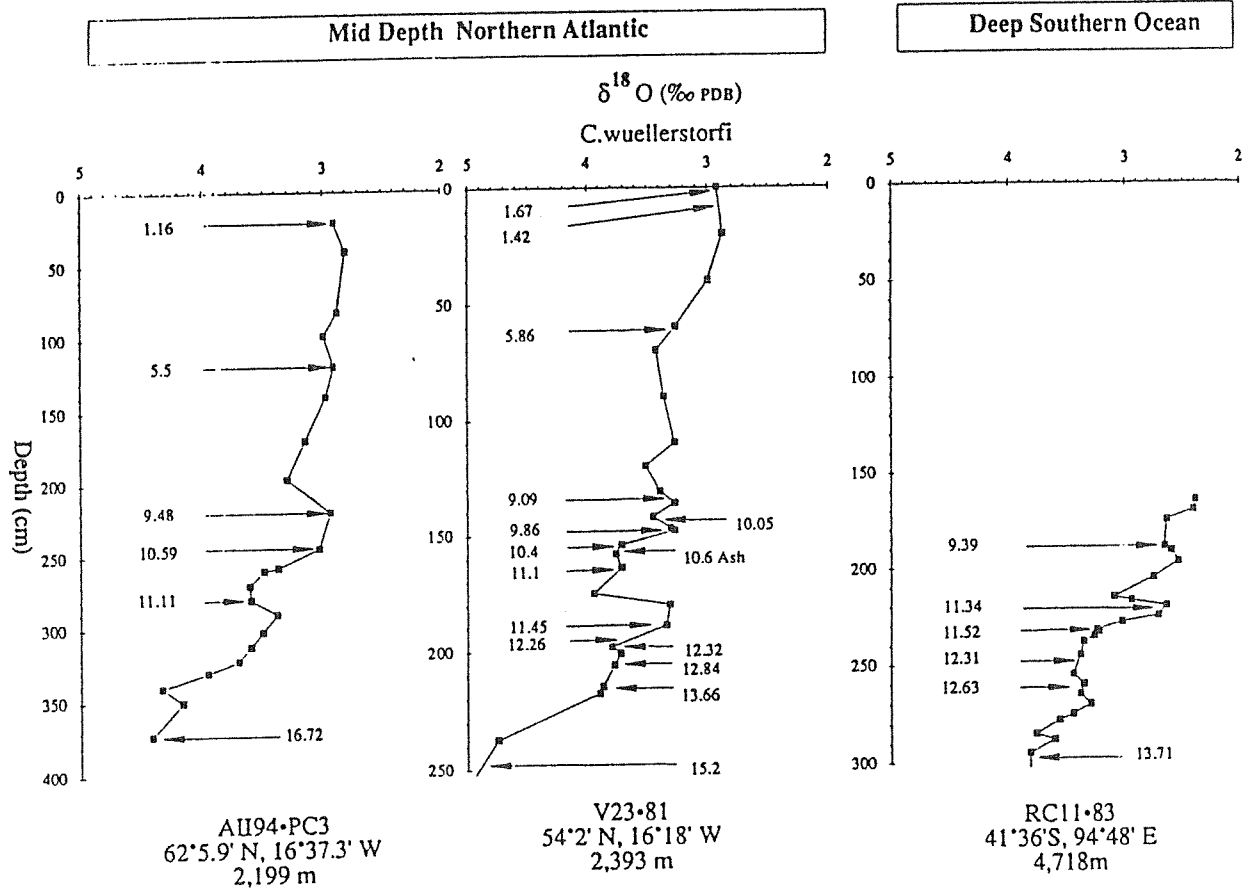


Figure 2: $\delta^{18}\text{O}$ records of the benthic foraminifer *Cibicidoides wuellerstorfi* from the mid-depth North Atlantic and deep Southern Ocean showing short-term depletion events (so-called "spikes" or "overshoots") before and after the Younger Dryas. $\delta^{18}\text{O}$ and ^{14}C results for V23-81 are from Jansen and Veum (1990) and Broecker et al (1988), respectively. $\delta^{18}\text{O}$ and ^{14}C results for AU94-PC3 are from D. Oppo, S. Lehman and L.D. Keigwin (unpublished data) and for RC11-83, from Charles and Fairbanks (1992). ^{14}C dates from the North Atlantic cores have been reservoir-corrected by 400 yrs to account for the modern air-sea activity difference. The Southern Ocean dates are corrected by 600 yrs.

depicted in Figure 3. Model parameters and a complete description of the model components are given in WS-93. Because the behavior of the model is germane to interpretation of model-diagnosed changes in oceanic $\delta^{18}\text{O}$, the results of WS-93 Younger Dryas simulations are outlined briefly below.

When the WS-93 ocean model is integrated to steady state with surface salinities and temperatures restored to observed values it produces a large-scale overturning circulation linking the Atlantic and Pacific through the Southern Ocean, consistent with the global conveyor circulation described by Gordon (1986) and Broecker (1991). Globally-integrated meridional heat transports and freshwater water fluxes produced by the model are in reasonable agreement

with observational estimates. In the Younger Dryas experiments, following initial integration of the ocean model to steady state, it was coupled to the atmospheric model and then exposed to a 10,000-year-long, time-varying meltwater input estimated from the radiocarbon dated record of deglacial sea-level rise (Fairbanks 1989). The geographic distribution of meltwater discharge is not known in detail, but based on glacial geologic reconstructions the Laurentide Ice Sheet produced about two-thirds of the total and a large fraction of this was routed through the Mississippi River and into the subtropical Atlantic (cf. Teller 1990, Keigwin et al 1991). All of the meltwater in the WS-93 and present experiments was therefore introduced to the North Atlantic between 20° and 32.5° N. Although not entirely realistic, this is an acceptable simplification given that our present aim is to evaluate mechanisms by which freshwater is incorporated into the deep ocean, rather than the sensitivity of the model circulation to changes in the location of meltwater input (cf. Maier-Reimer and Mikolajewicz 1989).

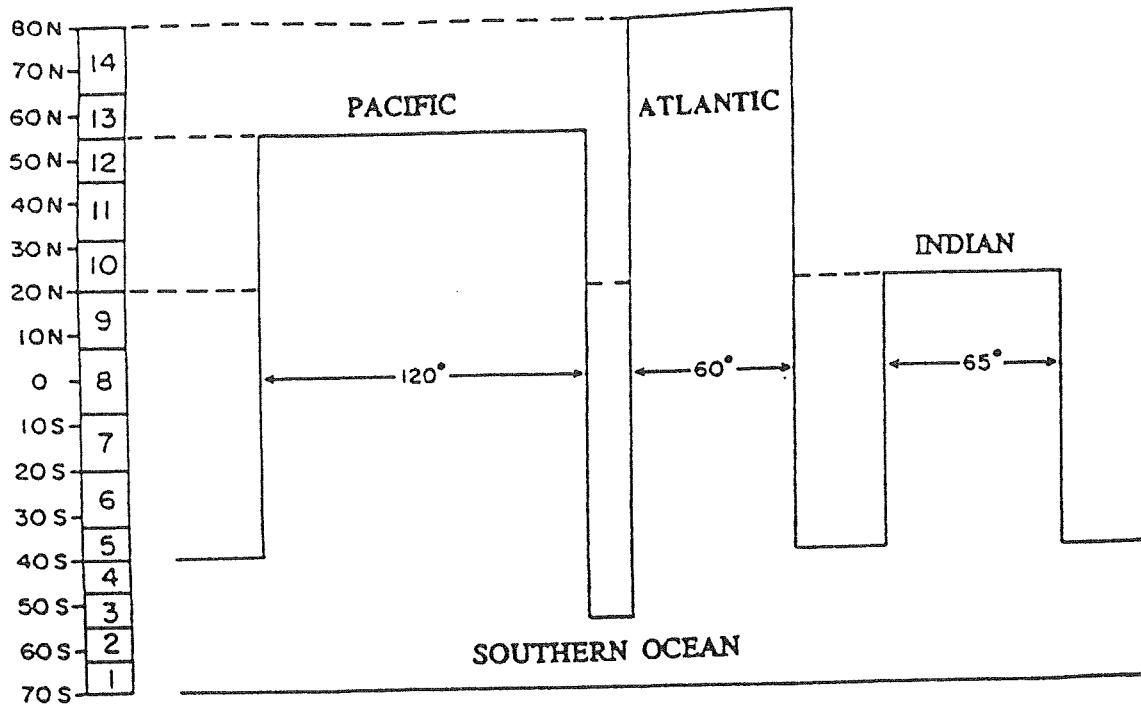


Figure 3: The idealized model representation of the global ocean. The Pacific, Atlantic and Indian Oceans are represented by 8, 10, and 5 latitude bands, respectively. Exchange between these basins occurs via the Southern Ocean, which occupies the southern-most 4 bands. Meltwater is introduced to the Atlantic at latitude band 10.

Figure 4 shows the model-diagnosed response of Atlantic heat transport (shown here as a proxy for the degree of Atlantic overturning) to realistic meltwater forcing for different estimates of the strength of the hydrologic cycle in the North Atlantic. When the WS-93 ocean model is restored everywhere to observed surface salinities prior to coupling with the atmospheric model, the overturning circulation collapsed soon after meltwater fluxes began to increase and failed to recover even as the flux of meltwater declined ($R=1$, Figure 4). However, when the model is integrated to steady state by restoring to specified surface water fluxes over the North Atlantic and restoring elsewhere to observed salinities, the sensitivity to meltwater forcing decreased substantially. For an extreme case ($R=0$, Figure 4) in which the freshwater balance in the North Atlantic is restored to actual observational estimates of precipitation minus evaporation (Baumgartner and Reichel 1976), the circulation is only slightly damped in response to the first meltwater peak and never collapses. The reason for this behavior is straightforward; restoring to estimates of precipitation minus evaporation produces model-diagnosed surface salinities in the northern Atlantic about 1 per mil greater than observed values. Due to the extra salt in the region of convection, greater freshening and thus more melting is needed in order to lower salinities to levels incompatible with convection. The excess salt also produces an ~50% increase in overturning compared to the case in which salinities are restored everywhere to observed values (cf. Figures 2 and 6 of SW-93). This reduces the residence time of surface waters in high latitudes and thus also the associated freshening, further reinforcing the strength of the overturning circulation.

One reason for the large discrepancy between diagnosed and observed salinities in the northern Atlantic, other than possible model error, is that run-off is not taken into account when restoring surface conditions to observational estimates of precipitation and evaporation. As the surface balance of precipitation, evaporation and run-off prior to the YD is not known, WS-93 freely tune the surface freshwater balance at integration by specifying a weighting factor between the cases $R=0$ and $R=1$ in order to achieve a circulation history that best matches the paleoceanographic record. As evident in Figure 4, the best fit is for $R=0.65$, or, in other words, for the case in which "run off" (or freshwater excess due to model error) is 65% of the model-predicted value ($R=1$).

In order to illustrate the phenomena that are most important in driving the model circulation into and out of the YD, the evolution of various parameters for the $R=0.65$ case is shown in Figure 5. Soon after the initial increase in meltwater flux, surface salinities begin to decline in the northern Atlantic, driving a gradual decrease in convection depth and overturning transport and thus in meridional heat flux and surface water temperature. The increased residence time of surface waters at latitudes of net precipitation ($> 40^\circ \text{ N}$) promotes freshening, further decreasing

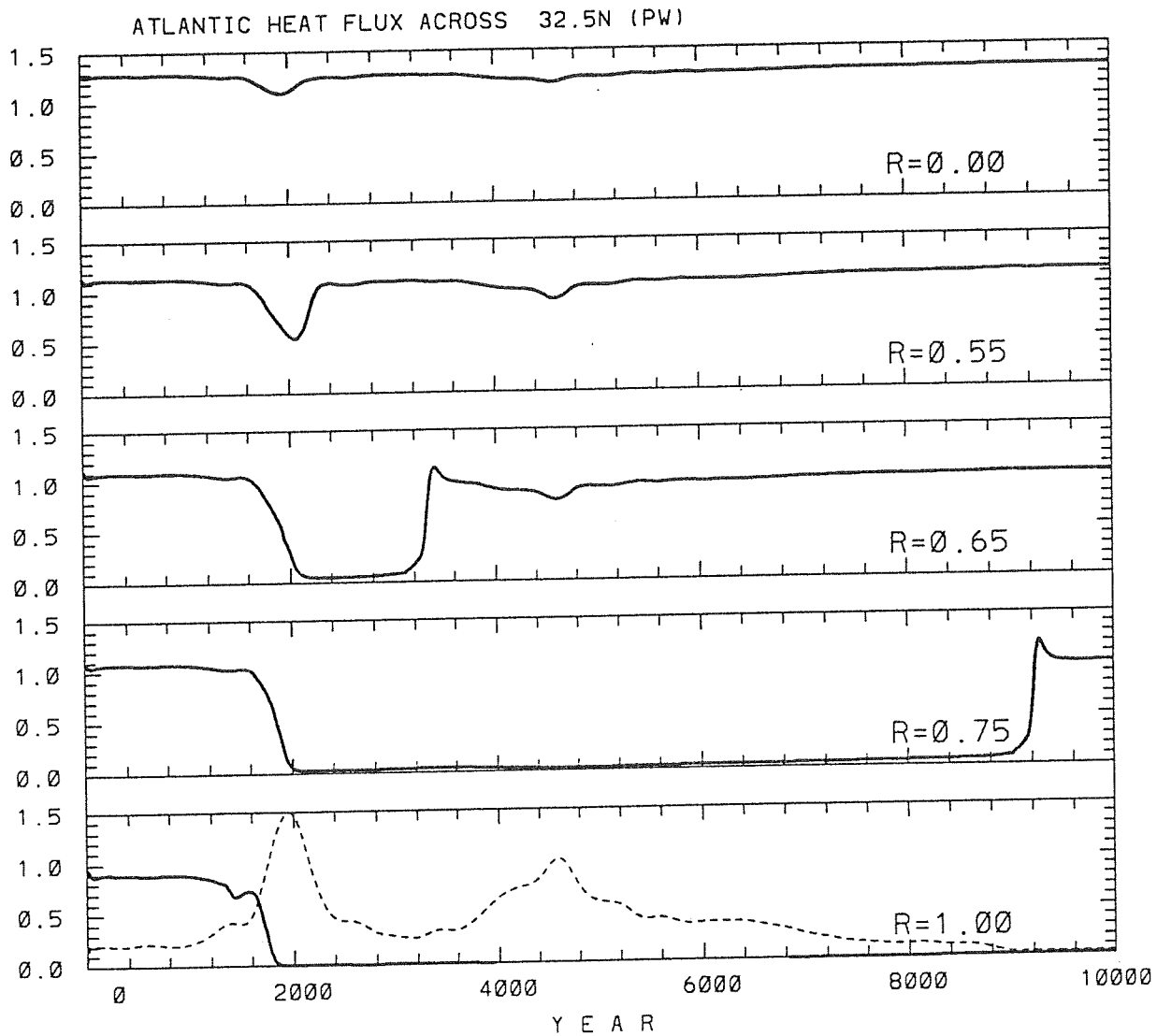


Figure 4: The history of heat flux across 32.5° N in the Atlantic basin for different specifications of the surface freshwater balance in the North Atlantic. In each case the model has been integrated to steady state under restoring boundary conditions, except in the North Atlantic basin, where the surface conditions are restored to specified freshwater fluxes (R). Larger values of R correspond to larger freshwater fluxes, as discussed in the text. At $t=0$ the ocean model is coupled to the atmospheric model and exposed to meltwater forcing. The meltwater is introduced between 20 and 32.5° N with an input schedule indicated by the broken line in the bottom panel (range = 0 - 0.45 Sv). The magnitude of the meltwater forcing is based on the rate of deglacial sea level change as estimated by Fairbanks (1989). Time moves from left to right (from the past to the present) with the meltwater peak at $t=2000$ corresponding to Fairbanks' MWP 1a, centered at ~ 12,000 reservoir-corrected ^{14}C yrs BP, and the peak at $t=4500$ corresponding to MWP 1b, centered at 9500 reservoir-corrected ^{14}C yrs BP. The best fit of the model circulation to the geologic record (Figure 1) is for $R=0.65$.

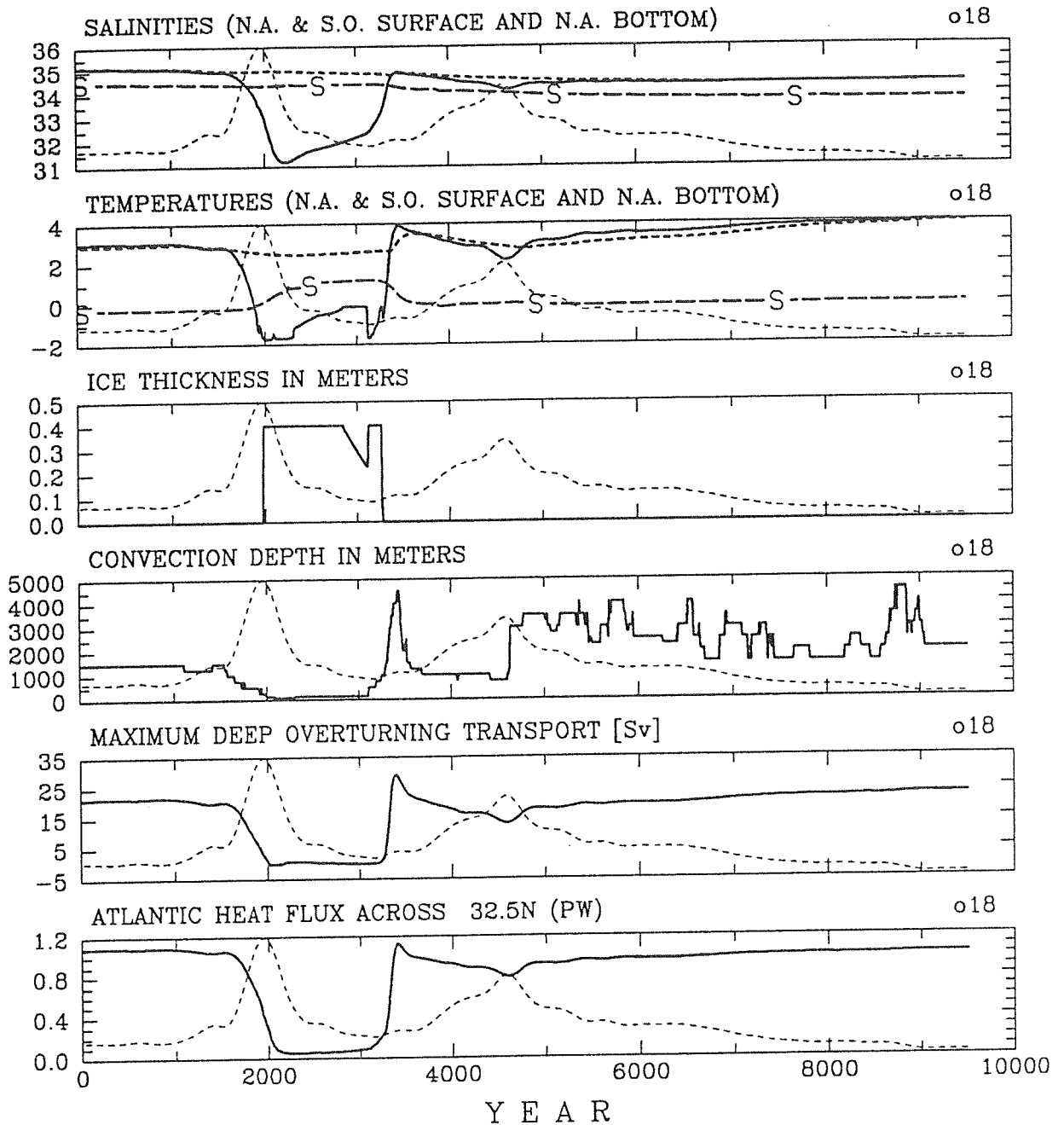


Figure 5. The evolution of the model properties for $R=0.65$. The light broken curve on each plot shows the schedule of meltwater input (range = 0 - 0.45 Sv). Solid lines refer to a) surface salinity, b) surface temperature, c) sea-ice thickness, and d) convection depth, all for the region north of 65° N in the Atlantic basin. Short-dashed lines in a) and b) are for potential temperature and salinity below 3000 m, and long-dashed lines for temperature and salinity at the surface of the Southern Ocean. Panel d) shows the history of the maximum values of the overturning stream function (in Sv) below 1000 m and north of 40° S in the Atlantic. The heat flux across 32.5° N in the Atlantic is also shown (e).

the overturning circulation and surface temperature. When temperatures fall to the freezing level, sea-ice grows rapidly in area and thickness, limiting further cooling of surface waters and damping the flux of ocean heat to the atmosphere. This enhances the buoyancy of surface waters and convection drops to negligible levels, bringing the overturning circulation to a state of collapse. This occurs at the time of peak meltwater flux, in accordance with geologic data in Figure 1. Once the overturning circulation has ceased, surface salinity quickly reaches minimum values. Although the residence time of surface waters at high latitudes remains elevated, salinity begins to rise gradually as a result of diffusion and wind-driven import of salt from latitudes of net evaporation and because the prescribed flux of meltwater has declined markedly. The gradual increase in salinity eventually permits shallow convection and the resultant mixing with saltier waters deeper in the water column further increases the salinity near the surface. A strong, positive feedback ensues in which both convection and salinity increase dramatically, bringing the circulation from the collapsed state into the overturning state.

The second meltwater pulse is not large enough to induce a second collapse of the circulation although overturning is damped slightly. As pointed out by WS-93, this is not due to preconditioning by the first meltwater peak. If the model is integrated to steady state for the case $R=0.65$ and exposed only to the second meltwater spike, the circulation is not perturbed. This indicates that for this specification of the surface freshwater balance, the WS-93 model exhibits a threshold in circulation response to meltwater forcing greater than ~ 0.2 Sv and less than ~ 0.45 Sv ($1 \text{ Sv} = 10^6 \text{ m}^3/\text{sec}$).

Isotope Experiments:

^{18}O is modeled as an independent passive tracer whose surface fluxes are set equal to half the surface fluxes of salt in order to reproduce the relationship between $\delta^{18}\text{O}^\dagger$ and salinity in the present-day ocean (cf. Figure 6a vs. 6b). Following integration to steady state, meltwater was added as in the earlier experiments, but with a prescribed oxygen isotopic composition of 40 ‰. This value was estimated based on a whole-ocean glacial- interglacial $\delta^{18}\text{O}$ shift of 1.2 per mil (Shackleton 1987; Labeyrie et al 1987; Broecker 1986) and a full glacial sea-level depression due to growth of continental ice sheets of 120 m (cf. Fairbanks 1989). Following addition of all of the meltwater, the model exhibits an average salinity decrease of ~ 0.8 per mil and an $\delta^{18}\text{O}$ decrease of ~ 1 per mil (Figure 7). These are $\sim 20\%$ lower than observed ($\delta^{18}\text{O}$) or calculated (S) changes deduced from the geologic record, due simply to the fact that the mean depth of the present-day ocean is 3.8 km, whereas the mean ocean depth in the model is 5 km. Although the magnitude of diagnosed $\delta^{18}\text{O}$ changes may therefore be underestimated by up to

$\dagger \delta^{18}\text{O} = (^{18}\text{O}/^{16}\text{O}_{\text{sample}}) / (^{18}\text{O}/^{16}\text{O}_{\text{std.}}) - 1$, in per mil

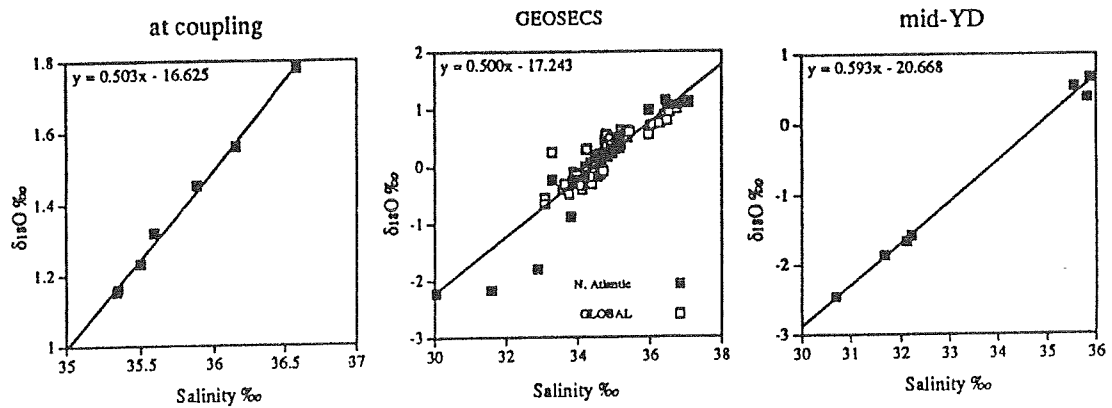


Figure 6: Relationship between salinity and $\delta^{18}\text{O}$ in surface waters in the ocean model at the time of coupling, before initiation of meltwater forcing (a). The surface fluxes of ^{18}O were set to half those of salt in order to reproduce the $\delta^{18}\text{O}$ -S relationship seen in the present-day surface ocean from GEOSECS data (b). Note that the slope of regression lines in a) and b) are the same, but that S and $\delta^{18}\text{O}$ in the present-day North Atlantic reach much lower values than seen in the model. The low values (below ~ 34.8 ‰) come from relatively fresh surface waters off Greenland. However, model results are zonal averages, and thus can not resolve the east-west asymmetry in S and $\delta^{18}\text{O}$ that characterizes the present-day northern North Atlantic. Furthermore, model salinities (and thus $\delta^{18}\text{O}$ values) at coupling are slightly higher than observed values because conditions at the surface of the North Atlantic were restored to a specified freshwater balance during integration, as discussed in the text. Shown in c) is the S - $\delta^{18}\text{O}$ mixing relationship diagnosed by the model in the middle of the YD ($t=2500$). The slope has increased slightly, and the freshwater ($S = 0$ ‰) end-member has become more depleted in ^{18}O due to the addition of meltwater.

20%, these differences do not affect the sense of time-dependent and spatial patterns of $\delta^{18}\text{O}$ produced by the model.

Figures 8 and 9 show the evolution of $\delta^{18}\text{O}$ of water ($\delta^{18}\text{O}_w$, solid lines) diagnosed by the model for a variety of locations and depths in the Atlantic. To enable comparison with the geologic record, the $\delta^{18}\text{O}$ of calcite ($\delta^{18}\text{O}_c$, dashed lines) is also shown. $\delta^{18}\text{O}_c$ was calculated from temperature and $\delta^{18}\text{O}_w$ using three different equations which describe the temperature dependence of oxygen isotope fractionation between water and calcite (those of O'Neil 1966, Shackleton 1974, Erez and Luz 1983). At the low temperatures of the deep ocean, the different equations yield significantly different values of $\delta^{18}\text{O}_c$ (cf. Zahn and Mix 1991). We therefore shifted the different $\delta^{18}\text{O}_c$ values by a constant factor to set them equal for a temperature of 4 °C (chosen because it is close to the average temperature of the deep ocean). At all locations, the time-dependent differences between values adjusted in this way are smaller than the typical analytical precision of the $\delta^{18}\text{O}_c$ measurement in foraminifera ($\sim \pm 0.1$ per mil). Adjusted

results for all three equations are plotted in Figures 8 and 9, but are indistinguishable. Although the adjustment factors obviously affect any attempt to compare absolute values of $\delta^{18}\text{O}_\text{C}$ diagnosed by the model with values measured in geologic samples, they do not interfere with our aim of evaluating time-dependent and spatial patterns of $\delta^{18}\text{O}_\text{C}$.

Temporal and spatial trends in Figures 8 and 9 lead to several important observations. First, time-dependent changes in $\delta^{18}\text{O}_\text{C}$ parallel changes in $\delta^{18}\text{O}_\text{W}$. Thus short-term changes in $\delta^{18}\text{O}_\text{C}$ appear to be governed primarily by penetration of ^{18}O -depleted surface waters into the deep ocean rather than by deepwater temperature. (Deepwater temperature changes are small and parallel overall changes in overturning circulation which are of much greater duration than the short-term changes in $\delta^{18}\text{O}_\text{W}$ and $\delta^{18}\text{O}_\text{C}$, cf. Figure 5b.) Second, short-term changes in $\delta^{18}\text{O}_\text{W}$ and $\delta^{18}\text{O}_\text{C}$ are more pronounced between 2.5 and 3.0 km water depth (Figure 9) than

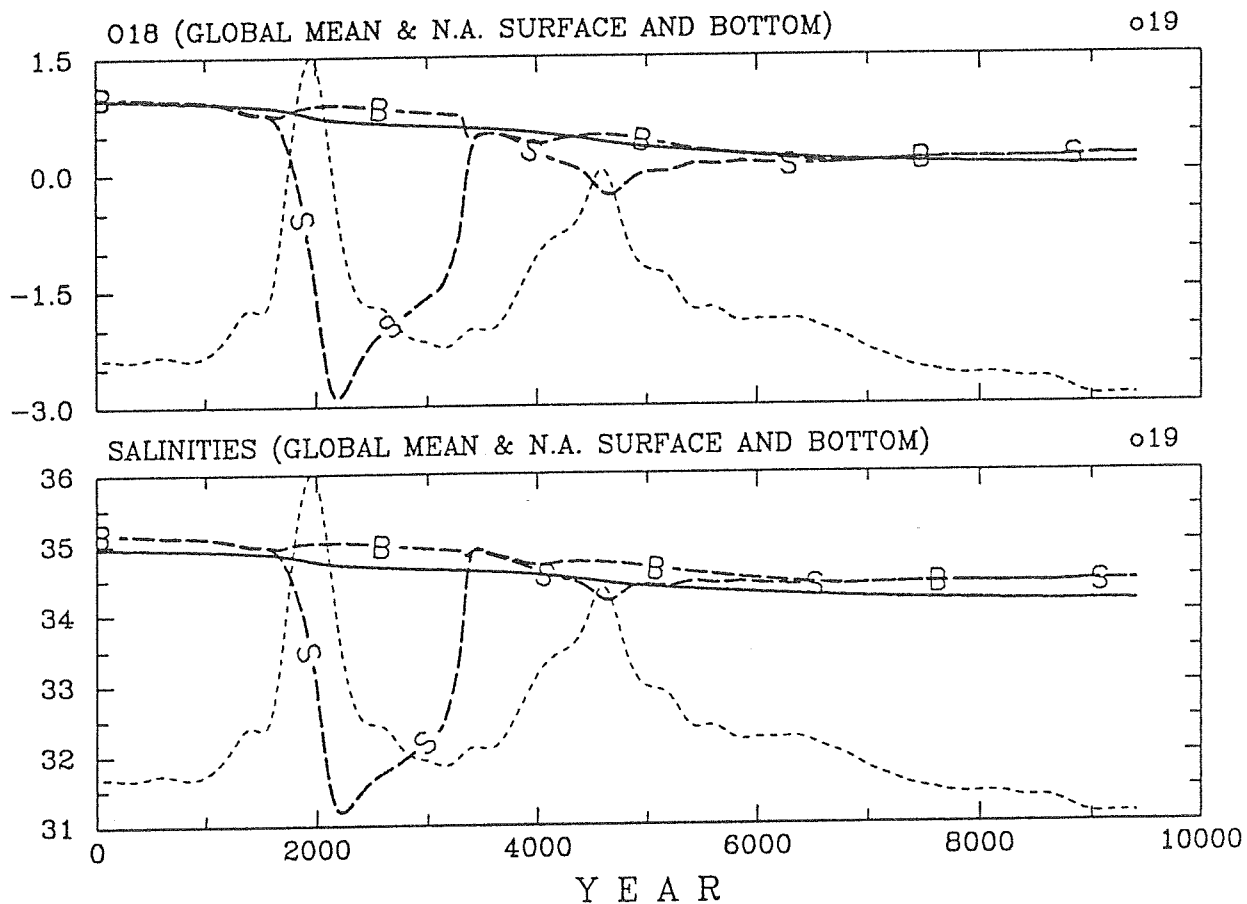


Figure 7: The evolution of model-diagnosed $\delta^{18}\text{O}_\text{W}$ a) and salinity b) at the surface (S) and below 3000 m (B) between 65° and 80°N in the Atlantic. Also shown (solid lines) is the evolution of global mean $\delta^{18}\text{O}_\text{W}$ and salinity. The schedule of meltwater forcing is indicated by the thin broken line (range = 0 - 0.45 Sv).

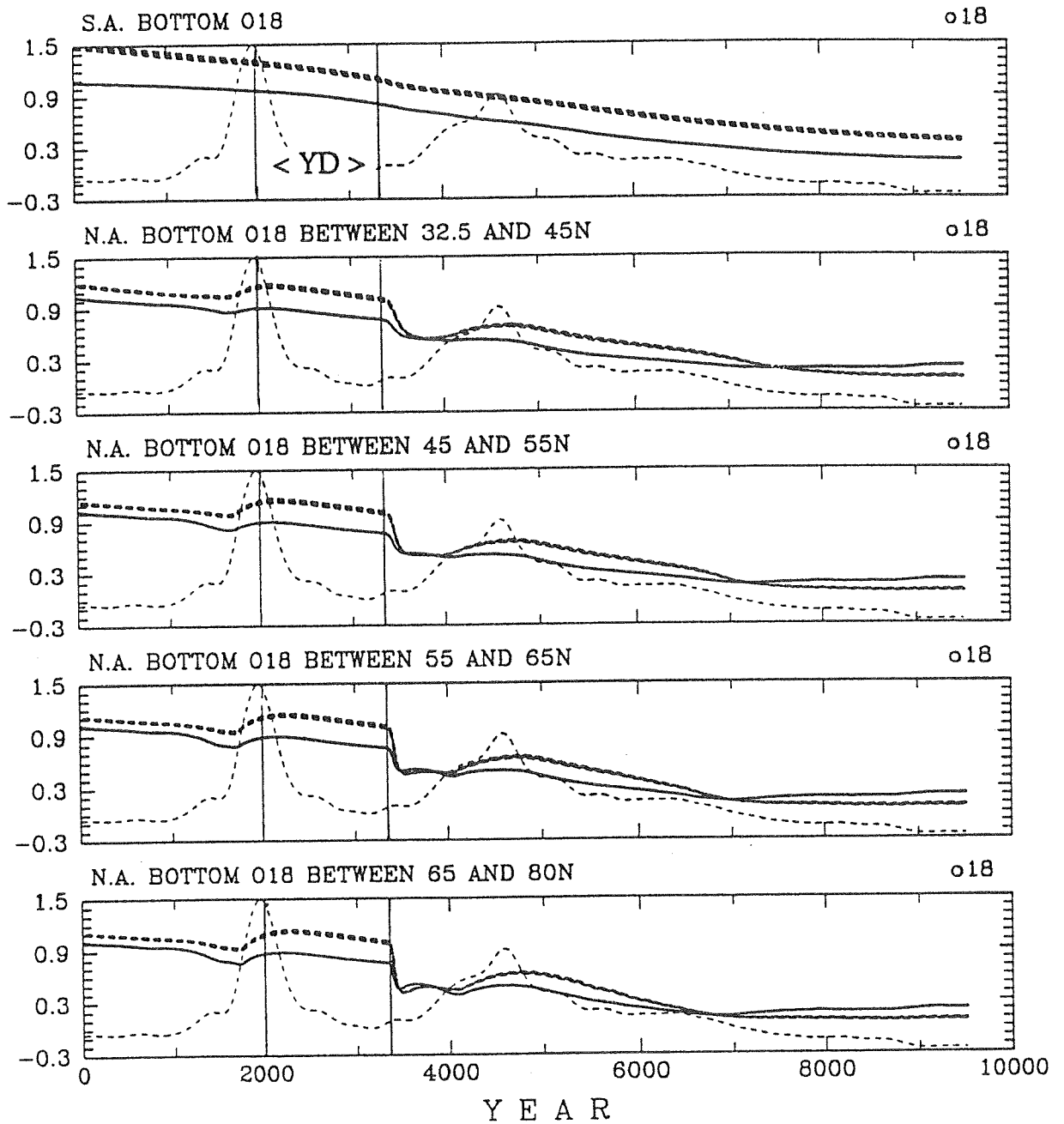


Figure 8: The evolution of model-diagnosed $\delta^{18}\text{O}_w$ (solid lines) and $\delta^{18}\text{O}_c$ (dashed lines) between 5000 and 4500 meters in the Atlantic. $\delta^{18}\text{O}_c$ was calculated from $\delta^{18}\text{O}_w$ and temperature, as discussed in the text. The vertical lines mark the beginning and end of the model's YD event during which the storage phase of our proposed "store and advect" cycle occurs.

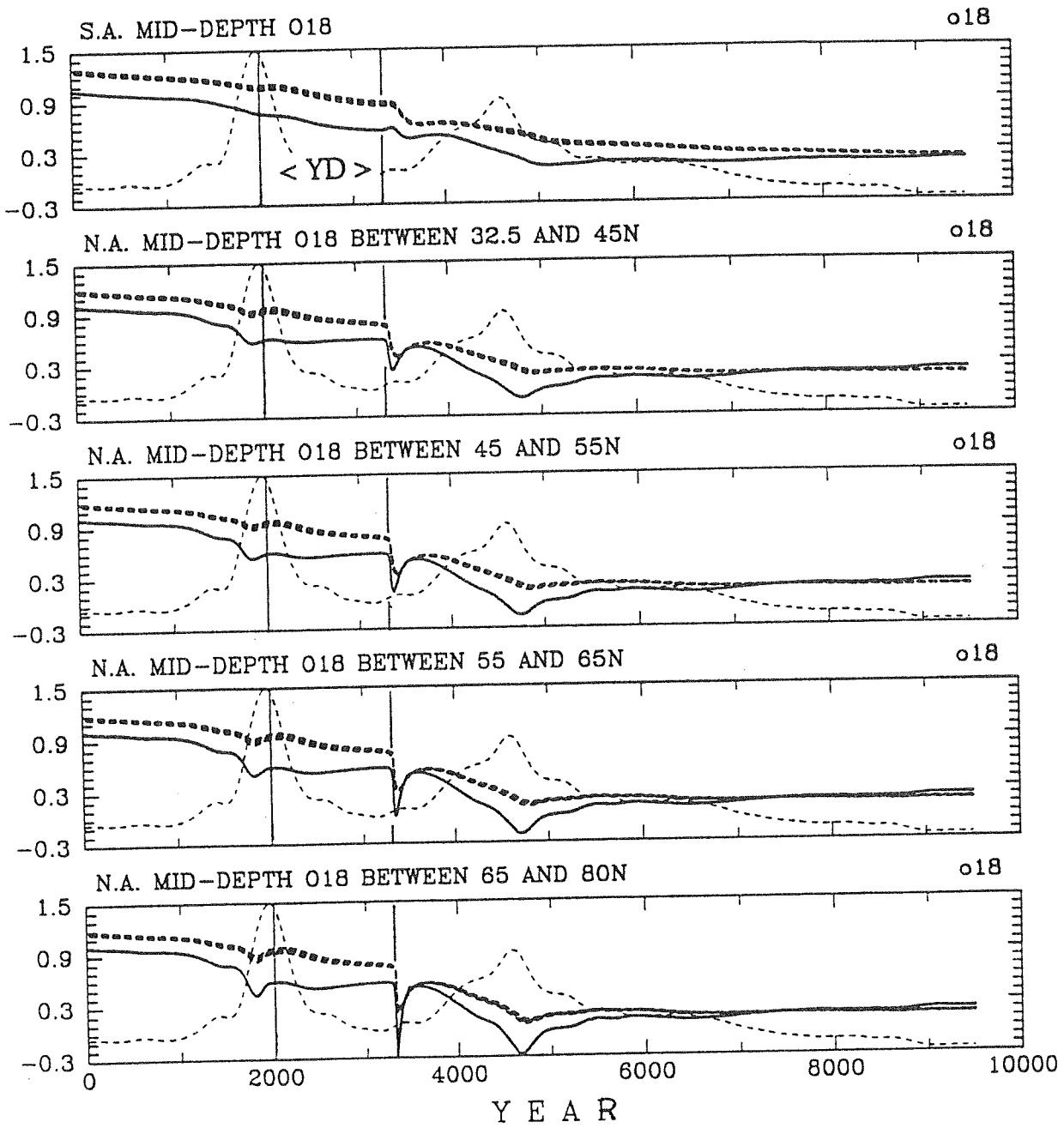


Figure 9: Same as in Figure 8, but for 3000 - 2500 meters depth.

between 4.5 and 5.0 km water depth (Figure 8). And, for a given depth, isotopic excursions are more pronounced in the northern North Atlantic than farther south. Both observations relate to the tendency for the rate of advection to exceed the rate of mixing by diffusion as the region of maximum overturning is approached. Such conditions predominate at mid-depth, close to the areas of deepwater formation in the northern Atlantic as seen in plots of the overturning stream function (Figure 10a and c). Third, at all locations except the deep South Atlantic (where the change in $\delta^{18}\text{O}$ with time is essentially linear), the largest and most abrupt short-term decreases in $\delta^{18}\text{O}$ are not associated with the times of greatest meltwater flux at the surface, but with the sudden recovery of the overturning circulation that defines the close of the model's YD event. In much of the deep Atlantic, the *only* significant shift in the rate of change of $\delta^{18}\text{O}$ occurs at this time. These abrupt $\delta^{18}\text{O}$ oscillations and steps result from the tendency of the model to sequester ^{18}O -depleted freshwater at the surface of the northern Atlantic during the YD and then to advect it quickly to depth as a result of the enhanced convection and overturning that marks the recovery of conveyor circulation (cf. Figure 5). Freshwater builds up during the YD, despite falling meltwater fluxes, because it is no longer removed by the overturning circulation. As noted earlier, there is a tendency for the wind-driven circulation to gradually erode the salinity deficit in the northern Atlantic during the YD. Although the change in salinity at the surface of the North Atlantic is critical to determining when the conveyor circulation will recover, North Atlantic surface waters are still greatly depleted in salt and ^{18}O with respect to the deep ocean at the time of recovery (Figure 7). Sudden transport of these ^{18}O -depleted surface waters into the ocean interior produces the large, short-term changes in $\delta^{18}\text{O}$ seen in the deep ocean.

In addition to the abrupt oscillation in the $\delta^{18}\text{O}$ of water and carbonate at the end of the model's YD event, smaller oscillations or steps occur at times of maximum meltwater water flux. These are most clearly evident in the mid-depth northern Atlantic, suggesting that meltwater has been advected to mid-depth as, or soon after, it reaches the ocean surface. However, significant changes at these times are not evident in the deep North Atlantic, nor in the deep and mid-depth South Atlantic. In fact, in the deep North Atlantic, $\delta^{18}\text{O}$ appears to increase slightly during the second meltwater pulse. This is a result of mixing with waters of the deep South Atlantic which have remained relatively enriched in ^{18}O . As the second meltwater pulse produces a slight decrease in the depth and strength of the overturning circulation (cf. Figure 5e), too little ^{18}O -depleted meltwater is advected into the deep North Atlantic to offset the effects of this mixing.

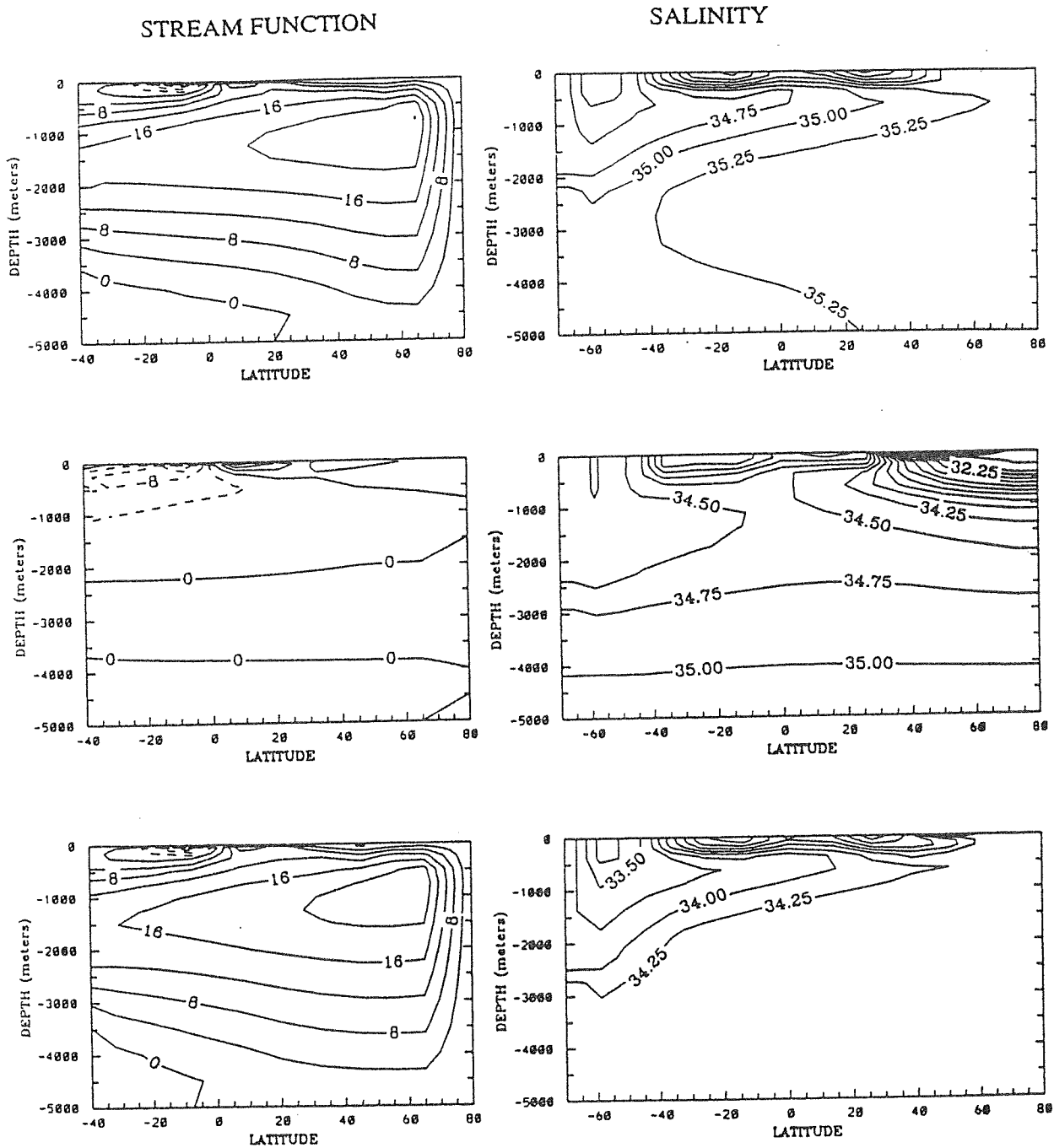


Figure 10: Cross sections of the overturning stream function (in Sv) and salinity (in ‰) in the Atlantic at the initiation of the meltwater input (a, at $t=0$), during the model's YD event (b, at $t=2500$) and at the end of the model run (c, at $t=10,000$). The pronounced northern halocline that develops during the model's YD event is clearly depicted in b). Note that the salinity plots extend to 70° S while the overturning stream function is shown only to 40° S.

Discussion of Results:

The rate at which $\delta^{18}\text{O}$ decreases in the deep ocean in these simulations depends largely on the strength of the overturning circulation and the availability of ^{18}O -depleted freshwater at the surface. We find that these conditions are satisfied under two rather different scenarios. The first is essentially as predicted at the outset; at times when prescribed meltwater fluxes are high and the conveyor circulation is still vigorous, ^{18}O -depleted meltwater is transmitted efficiently to at least mid-depth. The second scenario produces the most abrupt and pervasive decrease in deep ocean $\delta^{18}\text{O}$ at all depths and yet occurs when prescribed meltwater fluxes are at a minimum. As outlined earlier, this occurs in response to; 1) storage of ^{18}O -depleted freshwater at the surface of the North Atlantic when the overturning circulation collapses during the model's YD event, and 2) abrupt strengthening and deepening of the overturning circulation at the end of the YD. We refer to this as the "store and advect" scenario. Due to the timing (sensitivity) of circulation change with respect to the prescribed schedule of meltwater forcing, the deep ocean $\delta^{18}\text{O}$ responses associated with each of the two scenarios are slightly offset in Figures 8 and 9 and can thus be readily distinguished.

At the beginning of the model's YD event both the $\delta^{18}\text{O}$ and salinity of North Atlantic surface waters drop markedly as freshwater is no longer swept away and salt no longer swept in from lower latitudes by the overturning circulation (Figure 7). The increased residence time of surface waters north of the model's thermocline outcrop region, at latitudes where precipitation exceeds evaporation, leads quickly to the development of a strong halocline (Figure 10b). This behavior has been observed in association with the "conveyor off" state in many 3-D ocean models (cf. Bryan 1986, Manabe and Stouffer 1988). A similar feature is also suggested by salinity reconstructions for the last glacial maximum, when geochemical data indicate that the conveyor was much weaker than present (Duplessy et al 1991).

Once convection and overturning are re-initiated at the close of the YD, the ^{18}O -depleted halocline waters are folded rapidly into the deep ocean producing ^{18}O -depletion spikes and steps at depth. As a result of the strong positive feedback between increasing salinity and convection that occurs at the end of the model's YD event, overturning circulation and meridional heat flux actually overshoot later levels (Figure 5). Overshoots in air and sea temperatures are a common feature of cold-to-warm transitions in geologic record of circum-Atlantic climate (Atkinson et al 1987, Dansgaard et al 1989, Broecker 1992).

Both the storage of freshwater and the abrupt spin-up of the overturning circulation appear to be plausible phenomena based on their appearance in other numerical models and their probable equivalents in the geologic record. However, one may question the size of the salinity and $\delta^{18}\text{O}$ drop in the northern halocline produced by the model. In the early part of the YD,

both salinity and $\delta^{18}\text{O}$ have fallen by as much as 4 ‰ (Figure 7), almost twice as much as suggested by the planktonic $\delta^{18}\text{O}$ record of the northern Atlantic (cf. Duplessy et al 1992). One simple reason for possible exaggeration of the salinity and $\delta^{18}\text{O}$ drop in the model is that meridional mixing is portrayed by a single horizontal eddy diffusion coefficient (K_H) set to value of 500 m^2/sec . A more realistic parameterization of meridional mixing or the specification of a larger mixing coefficient might tend to diminish the salinity (and $\delta^{18}\text{O}$) contrast between the thermocline outcrop region and the northern halocline (Figure 10b)[†].

How much of the salinity and $\delta^{18}\text{O}$ drop that arises at the surface of the northern Atlantic during the model's YD event is due to continued melting vs. the climatological tendency of precipitation to exceed evaporation north of $\sim 40^\circ \text{N}$? The fact that surface salinities in the North Atlantic reach minimum values during the YD, despite prescribed meltwater fluxes that are less than half as large than either before or after suggests that the climatological forcing is dominant (cf. Figures 7 and 10). In fact, a similar reduction in surface salinity is seen in association with collapse of the overturning circulation in 3-D models which do not incorporate meltwater (Bryan 1986, Manabe and Stouffer 1988). The situation for $\delta^{18}\text{O}$ is somewhat different in that meltwater is approximately two times more depleted in ^{18}O than rainwater. The decrease in the $\delta^{18}\text{O}$ value of the freshwater end-member from -16 ‰ at coupling to -20 ‰ in the middle of the YD (Figures 6a vs. c) indicates that only about 17 % of the freshwater at the surface of the North Atlantic is of glacial origin. It is important to recall that all meltwater was introduced between 20° and 32.5°N in the present simulations. If some fraction of the meltwater were introduced north of the model's thermocline outcrop region the freshening and ^{18}O deficit that develops in the northern halocline during the YD would be larger and meltwater would drive a somewhat greater proportion of the observed $\delta^{18}\text{O}$ drop. An intriguing possibility raised by these results is that a significant fraction of the ^{18}O deficit constituting *short-term* depletion spikes in the deep ocean may be associated with stored rainwater whereas the gradual, *long-term* isotopic change in the deep ocean between the full glacial and the Holocene must be due to the transfer of ^{18}O -depleted water from the ice sheets to the oceans. The importance of meltwater, at least in this model, is that its input schedule appears to be instrumental in *pacing* the short-term isotopic changes through modulation of the overturning circulation.

[†] According to earlier experiments in which K_H was increased from 500 to 1000 m^2/sec , but which did not incorporate ^{18}O , the model behavior was the same as reported earlier, although the model-sensitivity to meltwater forcing decreased slightly. For $K_H = 1000 \text{ m}^2/\text{sec}$, the best-fit of the model circulation history to geologic data in Figure 1 was obtained for an R of 0.80 instead of 0.65. As this paper goes to press, ^{18}O simulations for $K_H = 1000 \text{ m}^2/\text{sec}$ and R = 0.80 are being run. We anticipate that a larger diffusion coefficient will reduce the previously observed depression of salinity and $\delta^{18}\text{O}$ within the northern halocline, but that this change will be small in comparison to the surface-to-deep $\delta^{18}\text{O}$ difference which ultimately drives the short-term decrease in deep ocean $\delta^{18}\text{O}$ values upon renewal of the conveyor circulation.

It should be recalled that the actual timing of circulation change with respect to the schedule of meltwater forcing was tuned at the outset through an adjustment of the surface freshwater balance. As outlined earlier, the tuning was aimed at reproducing the circulation history in Figure 1, in which (among other things) the conveyor remained in operation until the peak of the first meltwater pulse (cf. Figure 1). Our ability to trace the fate of freshwater from the surface into the deep ocean based on temporal and spatial $\delta^{18}\text{O}$ trends in Figures 8 and 9 provides some insight into how the thermohaline circulation might have accommodated such large fluxes of meltwater for so long. Because the overturning circulation quickly advects meltwater and rainwater to mid-depths, it acts to limit the accumulation of freshwater at the surface where it otherwise threatens convection.

Additional $\delta^{18}\text{O}$ - simulations for different specifications of the horizontal diffusion coefficient and locations of meltwater input will be needed in order to evaluate their influence on the size of the $\delta^{18}\text{O}$ drop in the northern halocline and to help clarify the relative importance of the "store and advect" mechanism vs. the real-time sinking of meltwater in driving changes in $\delta^{18}\text{O}$ of the deep ocean. Below we continue our discussion *on the assumption* that the "store and advect" behavior produced by the model is a plausible one and that it is an important process in producing time-dependent changes in $\delta^{18}\text{O}$ of the deep ocean. We take this liberty because if this is true, it carries important ramifications concerning the relationship between ice sheet melting, changes in surface and deep ocean $\delta^{18}\text{O}$, and changes in abyssal circulation deduced from sediments.

Storage and Advection of Freshwater and the $\delta^{18}\text{O}$ Record of the Last Deglaciation:

If the "store and advect" mechanism produced the major $\delta^{18}\text{O}$ spikes seen in sediments it must first be asked why the model produced only one such spike whereas the geologic data show at least two, one before and the other after the YD (cf. Figure 2). This is most likely because the model was initialized under conditions compatible with the "conveyor-on" state in an attempt to approximate the Allerød (pre-YD) circulation pattern. Following the first meltwater peak the model's conveyor circulation collapsed and then restored spontaneously, producing a single "store and advect" cycle. On the other hand, the deglacial ocean appears to have undergone two such cycles (cf. Figure 1). The first may have been associated with storage of freshwater during the glacial and with the subsequent renewal and strengthening of the overturning circulation at the beginning of the Bølling. The associated warming apparently lead to accelerated ice sheet melting (Lehman and Keigwin 1992, Charles and Fairbanks 1992). This, in turn, may have triggered a second "store and advect" cycle similar to the simulated one in which the conveyor circulation collapsed or weakened to produce the YD and then

spun-up again at the YD-Preboreal transition. Thus the "store and advect" behavior may have repeated itself during the deglaciation, accounting for the two main $\delta^{18}\text{O}$ decreases seen in sediments (Figure 2).

As the model produces only one "store and advect" cycle, an event-by-event comparison of the model results with the isotopic record in marine sediments is not possible. Instead, we use the few records which originally motivated this study (Figure 2) to evaluate the model output simply on the basis of the presence and form (step-like vs. spike-like) of short-term $\delta^{18}\text{O}$ changes diagnosed by the model.

In the North Atlantic, where the data coverage is most complete but still scant, the depth distribution of short-term $\delta^{18}\text{O}$ changes produced by the model and in the isotopic record of sediments are in general agreement. Both show larger changes at mid-depth than at deep locations: whereas North Atlantic records between 2 and 3 km water depth show overshoots (Figure 2), records from 4.5 km at Bermuda Rise fail to resolve overshoots despite very high deposition rates at that location (Boyle and Keigwin 1987, Keigwin et al 1991). In the model, and very probably in the real ocean, the overturning circulation tends to advect ^{18}O -depleted freshwater over and above the deepest part of the North Atlantic basin. The exception to this is the brief interval at the end of the model's YD event when the overturning cell approached the bottom of the basin, introducing freshwater and producing an ^{18}O -depletion step. Following this, $\delta^{18}\text{O}$ in the deep North Atlantic increased slightly. The increase results from mixing with relatively ^{18}O -rich waters of the deep South Atlantic (cf. Figure 8) and a simultaneous weakening of the overturning cell in response to the second meltwater pulse (cf. Figure 5). In the model, little ^{18}O -depleted freshwater has diffused or advected into the South Atlantic by the time of the second meltwater pulse, hence these waters remain relatively enriched in ^{18}O . However, in the present-day ocean, waters of the deep South Atlantic are relatively depleted in ^{18}O compared to deep waters of northern origin, due either to brine-rejection by sea ice[†] or incorporation of Antarctic meltwater during formation of Antarctic Bottom Water (Craig and Gordon 1965). These processes have not been incorporated into the present simulations.

The model produces no steps or overshoots in the deep South Atlantic whereas they are apparent at mid-depth. Presently there is only one high-resolution $\delta^{18}\text{O}$ record from the South Atlantic, located at 4.7 km water depth (Charles and Fairbanks 1992), and in contrast to the model prediction it shows pronounced overshoots (Figure 2c vs. Figure 8). Either the model has failed to advect northern-source water far enough south, or, in the real ocean, the overshoot was caused by downward mixing of local (Antarctic?) meltwater. Both are equally plausible. Our 2-D simulations do not produce a discrete, deep western boundary undercurrent so that

[†]Although the WS-93 model includes a sea ice formulation, it is not seasonal, and thus brine-rejection due to seasonal ice growth is not simulated.

^{18}O -depleted waters spread across the full breadth of the basin. The low- $\delta^{18}\text{O}$ anomaly would undoubtedly penetrate farther south if the portrayal of deep currents was more realistic (at the same time, the anomaly would weaken in the eastern basin of the North Atlantic). Second, meltwater was added only to the North Atlantic in the present simulation. It is possible that if some of the meltwater were added in the high-latitude South Atlantic, it may have been entrained by the deep mixing that characterizes the Southern Ocean.

No data-model comparison is possible for the Pacific due to the lack of suitable high resolution benthic $\delta^{18}\text{O}$ records. As the Pacific lies at the downstream end of the global-scale circulation, the model-simulated changes in $\delta^{18}\text{O}$ there (not shown) are muted in comparison to those of the South Atlantic. An evaluation of whether or not deep Pacific $\delta^{18}\text{O}$ values were affected by advection of ^{18}O -depleted deep waters from the Atlantic or by downward convection of local, ^{18}O -depleted surface water must await further study.

Conclusions:

According to our experiments, short-term decreases in $\delta^{18}\text{O}$ of the deep ocean can be traced to freshwater that has been stored at the ocean surface during periods of collapsed conveyor circulation. On the other hand, fluxes of meltwater are greatest when the conveyor is strong and appear to promote more gradual changes in the oxygen isotopic composition of the deep ocean. The freshwater storage produced by the model is similar to that suggested in a recent analysis of isotope and sea surface temperature data from the deglacial North Atlantic by Duplessy et al (1992) who show that the lowest surface salinities were achieved at times of greatest cooling. Correcting planktonic $\delta^{18}\text{O}_C$ data for temperature changes, they document strong $\delta^{18}\text{O}_W$ and salinity minima during the Oldest Dryas and then again during the YD. These events correspond to intervals of reduced ice sheet melting, as depicted in Figure 1, and with independent geochemical evidence of reduced formation of North Atlantic Deep Water (cf. Boyle and Keigwin 1987, Lehman et al 1991, Keigwin et al 1991). The primary conclusion reached by Duplessy et al (1992), who used an entirely different approach than the one used here, is identical to ours: the lowest salinity and $\delta^{18}\text{O}_W$ values at the surface of the northern North Atlantic were achieved when the conveyor was weakest and when ice sheet melting rates were smallest. Thus we speculate that the low-salinity and $-\delta^{18}\text{O}_W$ events documented by Duplessy et al (1992) represent the storage phases of our proposed "store and advect" cycles. Re-initiation of the conveyor circulation at the Oldest Dryas-Bølling and YD-Preboreal transitions then advected stored freshwater into the deep ocean, producing the brief decreases in $\delta^{18}\text{O}$ of benthic foraminifera before and after the YD. Although abrupt warming associated with the spin-up of the overturning circulation lead to accelerated ice sheet melting, the sweeping

action of the conveyor prolonged its ability to weather the growing fluxes of meltwater so that considerable melting was achieved both before and after the YD.

Returning to the questions posed at the outset, our modeling studies suggest that short-term decreases in $\delta^{18}\text{O}$ seen in benthic isotope records occur primarily as a result of brief but large decreases in $\delta^{18}\text{O}_w$ of the deep ocean, and not as a result of transient warmings of the deep ocean or significant changes in the relationship between $\delta^{18}\text{O}_w$ and salinity at deepwater source areas. However, contrary to our initial expectations, the largest and most pervasive short-term decreases in $\delta^{18}\text{O}$ at depth are not associated with the downward transport of meltwater while the conveyor circulation is strong. Rather, our simulations suggest that ^{18}O -depleted freshwater is stored at the surface of the northern Atlantic while the conveyor circulation is in the collapsed state and that it is subsequently folded into the deep ocean upon renewal of the circulation. Furthermore, much of the surface freshening and $\delta^{18}\text{O}_w$ decline appears to be due to accumulation of rainwater rather than meltwater. Regardless of which of these contributed most to the decline in salinity and $\delta^{18}\text{O}_w$ at the surface, our results suggest the timing of ^{18}O -depletion seen in high resolution benthic isotope records is controlled by the strength of the conveyor circulation. The fact that the extent of ^{18}O -depletion reaches a minimum during the YD provides additional evidence that the overturning circulation was restricted at that time in comparison to warm periods immediately before and after.

These findings suggest that circulation and climatology may have had a profound effect on the benthic and planktonic $\delta^{18}\text{O}$ record of the last and prior glacial terminations. They clearly warrant verification and further investigation in more realistic, 3-D models of the ocean and atmosphere.

Acknowledgments: E. Joynt III assisted with preparation of the figures and Dr. Delia Oppo kindly reviewed an early version of the manuscript. This work has been supported by NSF grant OCE91-819660. This is WHOI contribution no. 8387

References cited:

- Atkinson, T.C., K.R. Briffa, and G.R. Coope (1987). "The seasonal temperatures in Britain during the past 22,000 years, reconstructed using beetle remains." *Nature* 325: 587-592.
- Baumgartner, A. and E. Reichel (1975). *The World Water Balance*. New York, Elsevier. 179 pp.
- Boyle, E. A. and L. Keigwin (1987). "North Atlantic thermohaline circulation during the past 20,000 years linked to high-latitude surface temperature." *Nature* 330(6143): 35-40.
- Broecker, W. S. (1986). "Oxygen Isotope Constraints on Surface Ocean Temperatures." *Quaternary Research* 26(1): 121-134.

- Broecker, W. S. (1991). "The Great Ocean Conveyor." Oceanography 4(2): 79-89.
- Broecker, W. S. (1991). The Strength of the Nordic Heat Pump. The Last Deglaciation: Absolute and Radiocarbon Chronologies. Berlin, Springer-Verlag. 173-181.
- Broecker, W. S., M. Andree, et al. (1988). "The chronology of the last deglaciation: implications to the cause of the Younger Dryas event." Paleoceanography 3(1): 1-19.
- Broecker, W. S., T.-H. Peng, et al. (1990). "The magnitude of global fresh-water transports of importance to ocean circulation." Climate Dynamics 4: 73-79.
- Bryan, F. (1986). "High-latitude salinity effects and interhemisphere thermohaline circulations." Nature 323: 301-304.
- Charles, C. D. and R. G. Fairbanks (1992). "Evidence from Southern Ocean sediments for the effect of North Atlantic deep-water flux on climate." Nature 355: 416-419.
- Craig, H. and L. I. Gordon (1965). Deuterium and oxygen-18 variations in the ocean and the atmosphere: Stable isotopes in oceanographic studies and paleotemperatures. Third Spoleto Conference, Spoleto, Italy, Sischi and Figili.
- Dansgaard, W., H.B. Clausen, et al. (1982). "A new Greenland deep ice core." Science 218: 1273-1277.
- Dansgaard, W., J. W. C. White, et al. (1989). "The abrupt termination of the Younger Dryas climate event." Nature 339: 532-533.
- Duplessy, J. C., G. Delibrias, et al. (1981). "Deglacial warming of the Northeastern Atlantic Ocean: correlation with the Paleoclimatic evolution of the European continent." Palaeogeography, Palaeoclimatology, Palaeoecology 35: 121-144.
- Duplessy, J. C., L. Labeyrie, et al. (1992). "Changes in surface salinity of the North Atlantic Ocean during the last deglaciation." Nature 358: 485-488.
- Duplessy, J. C., L. Labeyrie, et al. (1991). "Surface salinity reconstruction of the North Atlantic Ocean during the last glacial maximum." Oceanologica Acta 14: 311-324.
- Erez, J. and B. Luz (1983). "Experimental paleotemperature equation for planktonic foraminifera." Geochimica et Cosmochimica Acta 47: 1025-1031.
- Fairbanks, R. G. (1989). "Glacio-eustatic sea level record 0-17,000 years before present: influence of glacial melting rates on Younger Dryas event and deep ocean circulation." Nature 342: 637-642.
- Gordon, A. L. (1986). "Interocean Exchange of Thermohaline Water." Journal of Geophysical Research 91(C4): 5037-5046.
- Jansen, E. and T. Veum (1990). "Evidence for two-step deglaciation and its impact on North Atlantic deep-water circulation." Nature 343: 612-616.
- Keigwin, L. D., G. A. Jones, et al. (1991). "Deglacial Meltwater Discharge, North Atlantic Deep Circulation, and Abrupt Climate Change." Journal of Geophysical Research 96(C9): 16811-16826.

- Labeyrie, L. D., J. C. Duplessy, et al. (1987). "Variations in mode of formation and temperature of oceanic deep waters over the past 125000 years." Nature 327: 477-482.
- Lehman, S. J. and L. D. Keigwin (1992). "Sudden changes in North Atlantic circulation during the last deglaciation." Nature 356: 757-762.
- Maier-Reimer, E. and U. Mikolajewicz (1989). Experiments with an OGCM on the cause of the Younger Dryas. Max-Planck-Institut für Meteorologie.
- Manabe, S. and R. J. Stouffer (1988). "Two Stable Equilibria of a Coupled Ocean-Atmosphere Model." Journal of Climate 1: 841-866.
- O'Neil, J. R., R. N. Clayton, et al. (1969). "Oxygen isotope fractionation in divalent metal carbonates." Journal of Chemical Physics, 51: 5547-5558.
- Semtner, A. J. (1976). "A model for the thermodynamic growth of sea ice in numerical investigations of climate." Journal of Physical Oceanography 6: 379-389.
- Shackleton, N. J. (1987). "Oxygen Isotopes, Ice Volume and Sea Level." Quaternary Science Reviews 6: 183-190.
- Stocker, T. F., D. G. Wright, et al. (1992). "A zonally averaged, coupled ocean-atmosphere model for paleoclimate studies." Journal of Climate 5: 773-797.
- Teller, J. T. (1990). "Volume and Routing of Late-Glacial Runoff from the Southern Laurentide Ice Sheet." Quaternary Research 34: 12-23.
- Winton, M. and E. S. Sarachik (1993 in press). "Thermohaline Oscillations Induced by Strong Steady State Forcing of Ocean General Circulation Models." Journal of Physical Oceanography :
- Wright, D. G. and T. F. Stocker (1991). "A Zonally Averaged Ocean Model for the Thermohaline Circulation. Part I: Model Development and Flow Dynamics." Journal of Physical Oceanography 21: 1713-1724.
- Wright, D. S. and T. F. Stocker (1993 in press). "Younger Dryas Experiments.", this volume.
- Zahn, R. (1992). "Deep ocean circulation puzzle." Nature 356: 744-746.
- Zahn, R. and A. C. Mix (1991). "Benthic Foraminiferal $d^{18}O$ in the Ocean's Temperature-salinity-density Field: Constraints on Ice Age Thermohaline Circulation." Paleoceanography 6(1): 1-20.